Advanced Composite Materials
Publication details, including instructions for authors and subscription information:
http://www.tandfonline.com/loi/tacm20

Mode II delamination in ± laminates: Analysis and optimisation

A. Laksimi , A. Ahmed Benyahia , X. L. Gong & S. Benmedakhene

Version of record first published: 02 Apr 2012.

To cite this article: A. Laksimi , A. Ahmed Benyahia , X. L. Gong & S. Benmedakhene (2000): Mode II delamination in ± laminates: Analysis and optimisation , Advanced Composite Materials, 9:3, 207-221

To link to this article: http://dx.doi.org/10.1163/15685510051033386

Adv. Composite Mater., Vol. 9, No. 3, pp. 207–221 (2000)

Mode II delamination in $\pm\theta$ laminates: Analysis and optimisation

A. LAKSIMI [1], A. AHMED BENYAHIA [1], X. L. GONG [2] and S. BENMEDAKHENE [1]

[1] *LG2mS UPRES-A6066 Université de Technologie de Compiègne (UTC), B.P. 20529, 60205 Compiègne, France*
E-mail: Abdelouahed.Laksimi@utc.fr
[2] *LASMIS, GSM, Université de Technologie de Troyes (UTT), 12, rue Marie Curie B.P. 2060, 10010 Troyes cedex, France*

Received 1 January 2000; accepted 21 March 2000

Abstract—The literature concerning $\pm\theta$ laminates under mode II (propagation mode) loading encounters a difficulty in calculation of the structural dimensions. Indeed, it is rare to have a specimen geometry which fully satisfies the conditions for application of the Linear Elastic Fracture Mechanics (LEFM). Thus, the aim of this work is the optimisation of the specimen geometry which allows the characterisation of mode II by the approach of the LEFM concept. The results obtained show an interaction between the geometrical characteristics of the specimen (thickness h), the angle of orientation of the plies (θ) and the characterisation of delamination. The experimental results are in good agreement with the analytical predictions. The use of the acoustic emission allows us to observe that delamination is only one final stage in a process of damage which starts well before.

Keywords: Laminates ($\pm\theta$); mode II; specimen optimisation; fracture; stress analysis.

1. INTRODUCTION

The majority of work in the literature reporting on delamination in mode II by flexion in multidirectional laminates use sequences of stacking consolidated by plies with 0°. This sequence consolidation of stratification makes it possible to avoid the bifurcation phenomenon but does not reflect the case of the structures $[\pm\theta]$ used in industry.

When $\pm\theta$ laminates are tested, the encountered problem is that cracks may deviate from the original crack plane, invalidating the fracture mechanics approach. Also, low specimen stiffness may result in large displacements and non-linear behaviour, especially in mode II loading.

Moreover, the comparisons are made between the values of the energy release rate for various interfaces without taking account of the sequences of stacking. However,

the plies with the large angles (especially the 90°) have transverse fractures even if they are not adjacent to the plane of propagation of the crack. Thus, the energy dissipated in these plies is taken into account in the calculation of the energy release rate although it is not dissipated at the crack tip. According to some authors [1–3], the bifurcation phenomenon is due to an edge effect. Few studies concerning mode II loading use the linear elastic fracture mechanic concepts to obtain the energy release rate G_{II}. It is indeed about an interaction between the angle of ply orientation, θ, the geometrical characteristics (thickness h) of the specimen and the energy release rate G_{II}. Thus, the study of mode II in the case of $\pm\theta$ laminates requires a preliminary adaptation thickness of the specimen according to the angle θ. It concerns the characterisation of the fracture in a mode of pure shearing. The difficulty in the design of a mode II specimen is to avoid any cracking by opening without causing excessive friction between the two faces of the crack.

Several specimen types was developed to characterise mode II. They concern mainly the three point bending test and cantilever flexure, respectively ENF (End Notch Flexure) and ELS (End Load Split).

However, the specimen geometry must take into account the length L, the thickness h and crack length a. The method of compliance requires a significant length to vary the size of the initial crack a_0. However, certain composite materials, which have a rather weak Young's modulus (for example, glass-epoxy) associated to a significant length L, introduce a large displacement before the starting of delamination. This study leads to a better understanding the behaviour of the sequence $\pm\theta$ laminates and gives an optimised method for this specimen type under a mode II loading.

2. EXPERIMENTAL ANALYSIS

2.1. Material and experimental conditions

The material used in this study was an E-glass/M10-epoxy composite. The fibre volume fraction was about 52%. The test specimens were cut from 300 mm by 300 mm plates. A Teflon film (30 μm thikness) is incorporated at the mid-plane to initiate the delamination (Fig. 1). The thickness of 4.8 mm is composed of 16 plies. The plates were cured in an air press according to the manufacturer's recommended cure cycle (3 bars for 1 h at 120°C). Four configurations $[(+\theta/-\theta)_{2s}]_s$ were selected with angles: $\theta = 15°$, 30°, 45° and 60°. The starter film is inserted in the interface between θ/θ laminae at the mid-plane of the stacking sequence: $(+\theta/-\theta/+\theta/-\theta/-\theta/+\theta/-\theta/+\theta//+\theta/-\theta/+\theta/-\theta/-\theta/+\theta/-\theta/+\theta)$. In order to study the shearing mode, two specimen types (ELS and ENF) were used (Fig. 1) and dimensions are indicated in Table 1.

Each specimen was instrumented by a receptor of acoustic emission and strain gauges were placed in the surface of the specimens, as indicated in Fig. 1. The specimens were loaded in displacement control at a constant rate of 0.5 mm/min in order to better see the occurrence of the damage mechanisms.

Table 1.
Geometrical characteristics of specimens ELS and ENF

Specimens	Width B (mm)	Length L (mm)	Total thickness 2 h (mm)	Ratio a_0/L
ELS	20	60	4.8	$0.4 < a_0/L < 0.7$
ENF	20	50	4.8	$0.4 < a_0/L < 0.7$

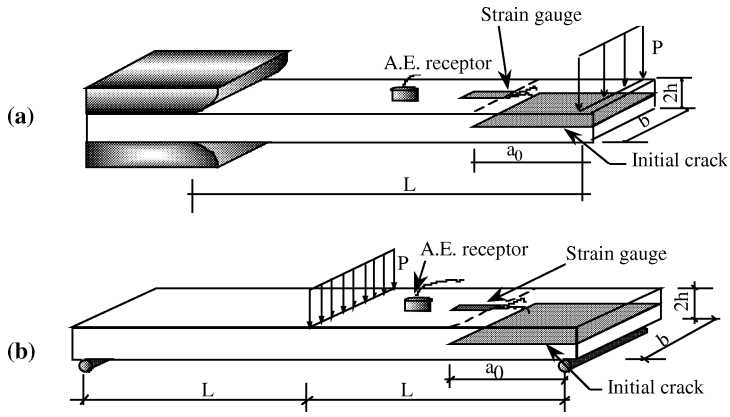

Figure 1. Specimens (a) ELS (b) ENF.

2.2. Analysis of the mechanical behaviour according to the angle θ

The shape of the load–displacement curves depends on the laminate sequence and on the ratio a_0/L (a_0: initial crack length, L: specimen useful length, Fig. 2). For a same ratio a_0/L, the elastic linear domain becomes increasingly short when the angle θ increases. The domain of non-linearity becomes wider. The modulus of elasticity as well as fracture strength of the plies in the flexure decreases with the increase in θ. The graphs in Fig. 2 show the existence of two critical points: the end point of linearity (P_{NL}) and the point corresponding to the maximal loading ($P_{\max}$). It is thus interesting to know what occurs at these two points in terms of mechanical resistance of the material.

The mechanical approach is done by the determination of the energy release rate by using the compliance method:

$$G_{\mathrm{II}} = \frac{P^2 \partial c}{2B \partial a}, \tag{1}$$

P is the applied load P_{NL} or $P_{\max}$; B is the specimen width; and $\partial c/\partial a$ is a partial derivative of compliance with respect to the crack length. Four specimens for each laminate were tested.

The calibration of compliance is done according to the law $C = \alpha + \beta a^3$ [10], α and β are material parameters determined with different ratio a_0/L of specimens. The values obtained for the four configurations are summarised in Table 2.

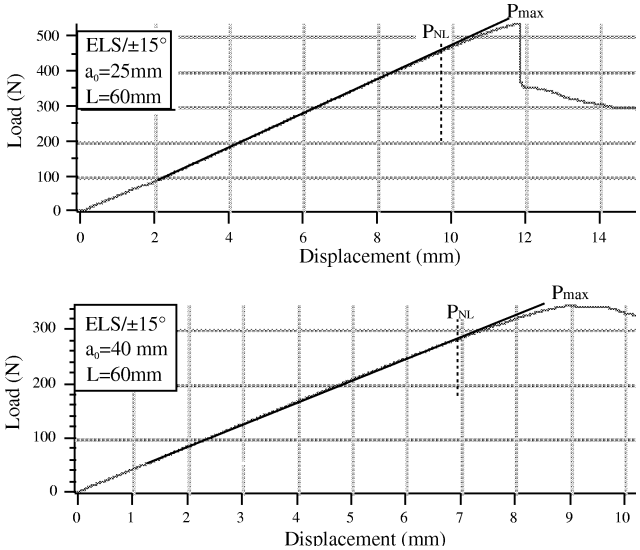

Figure 2. Evolution of the curves of load–displacement according to the ratio a_0/L.

Table 2.
Compliance parameters α and β according to θ

Laminate	(±15°)	(±30°)	(±45°)	(±60°)
$\alpha \times 10^{-2}$ (mm/N)	1.42	2.21	1.80	2.36
$\beta \times 10^{-7}$ (1/N · mm^2)	1.55	1.85	3.56	7.10

The results of the energy release rate G_{II} corresponding to the loads P_{NL} and $P_{\max}$ are summarised in Table 3.

The $G_{\mathrm{II}\max}$ values corresponding to the sequence $\theta = \pm 60°$ could not be given because of the specimen fracture by flexure without delamination. All the configurations seem to have fracture energies ($G_{\mathrm{II}\max}$) which converge towards a value approximately 2 kJ/m^2. On the other hand, the $G_{\mathrm{II.NL}}$ values are rather sensitive to the variation of the angle θ. Whatever the ratio a_0/L, $G_{\mathrm{II.NL}}$ decreases when θ increases. The comparison of the ratios $G_{\mathrm{II}}^{\mathrm{NL}}/(G_{\mathrm{II}\max})$ shows that they decrease significantly with the increase of the angle θ (Table 4). The sequences with weak angles are more resistant but become more vulnerable than the sequences with greater angles because the maximal loading to fracture is reached shortly after P_{NL}.

All the $G_{\mathrm{II}\max}$ values are lower than the values characterising delamination in pure mode II of glass-epoxy material (2.5 kJ/m^2). It means that the fracture initiation is done by a damage mode requiring less work of the external loading.

The $G_{\mathrm{II.NL}}$values correspond to the beginning of the non-linear behaviour of the material. This is not necessarily due to the beginning of damage. Large displacements can generate this behaviour type which necessitates the use of acoustic emission in order to highlight the occurrence of the damage.

Table 3.
Energy release rate of specimen ELS. (Standard deviations are given in parentheses)

Sequences	a_0/L	$G_{\text{II.NL}}$ (kJ/m^2)	$G_{\text{II.max}}$ (kJ/m^2)
0°	0.4	2.01 (0.15)	2.63 (0.28)
	0.5	1.86 (0.18)	2.43 (0.21)
	0.6	1.87 (0.11)	2.45 (0.19)
±15°	0.4	1.44 (0.12)	1.91 (0.13)
	0.5	1.55 (0.13)	2.07 (0.14)
	0.6	1.54 (0.11)	1.99 (0.15)
	0.7	1.52 (0.09)	2.13 (0.12)
±30°	0.4	0.65 (0.07)	1.51 (0.09)
	0.5	0.87 (0.09)	1.96 (0.12)
	0.6	1.20 (0.09)	2.10 (0.08)
	0.7	0.78 (0.07)	1.89 (0.08)
±45°	0.4	0.22 (0.02)	0.92 (0.04)
	0.5	0.34 (0.03)	1.51 (0.08)
	0.6	0.23 (0.01)	1.38 (0.08)
	0.7	0.29 (0.02)	1.16 (0.06)
±60°	0.4	—	—
	0.5	—	—
	0.6	0.24 (0.02)	—
	0.7	0.21 (0.03)	—

Table 4.
Ratio $G_{\text{IINL}}/G_{\text{IIC}}$ for specimen ELS

a_0/L	$G_{\text{IINL}}/G_{\text{IIC}}$			
	0°	±15°	±30°	±45
0.4	0.76	0.75	0.43	0.31
0.5	0.77	0.75	0.44	0.23
0.6	0.76	0.77	0.56	0.17
0.7	—	0.72	0.41	0.25

3. IDENTIFICATION OF THE START OF DELAMINATION

For specimens ELS or ENF, the load−displacement curves have relatively significant non-linearity especially for the great angles. This poses the problem of the choice of G_{IIC} for the calculation of the structure's dimensions. The material tenacity can be over-estimated or under-estimated according to the point of initiation considered, because the difference between $G_{\text{II.NL}}$ and $G_{\text{II max}}$ can be very high especially for significant angles θ. Carlsson *et al*. [6] proposed taking an intermediate point using a correction factor. However, this approach applies only to one material having a very ductile resin. It is not the case for the material used in this study. The technique of the acoustic emission is adequate to answer this problem by de-

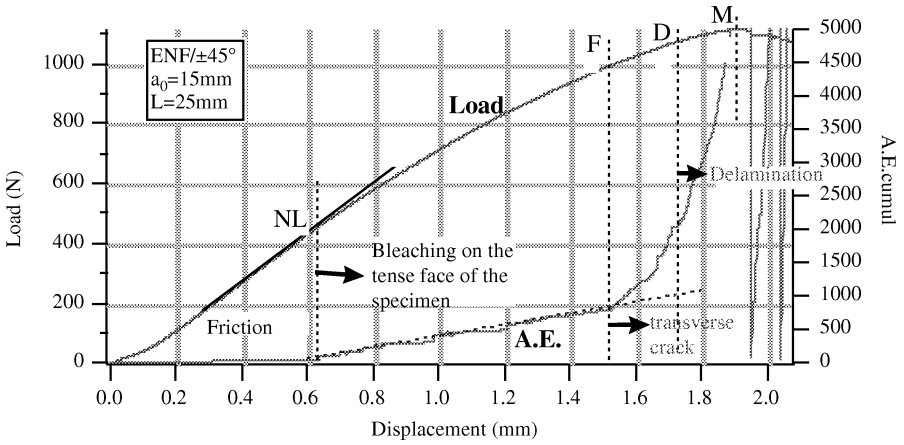

Figure 3. Load–displacement and cumulative A.E. for ±45°.

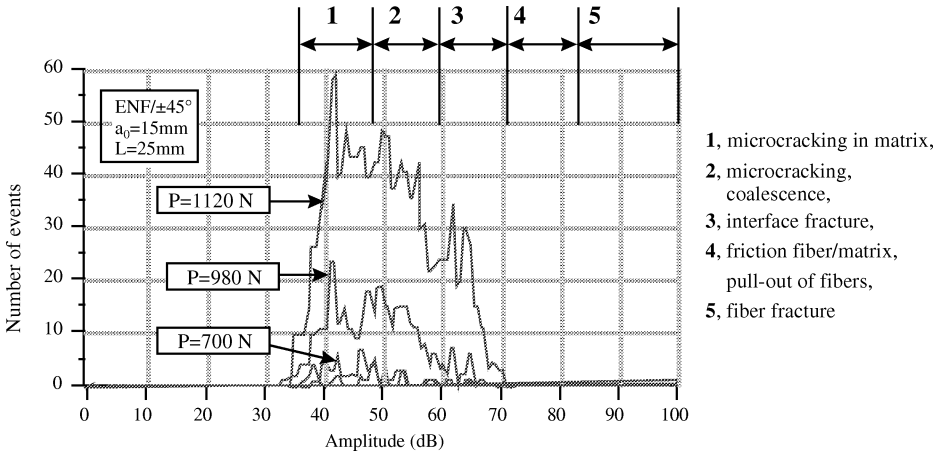

Figure 4. Amplitude distribution for ±45°.

tecting different phases of damage mechanisms. The characteristics of the acoustic emission (A.E.) system are the following:

- Preamplifier gain: 39 dB.
- Threshold setting: 39 dB for this study.
- Bandwidth: 100–400 kHz.
- Piezoelectric sensor broad band: 200 kHz–1 MHz.

Figure 3 shows evolution of the load-displacement curve and the cumulative A.E.

Previous works [7, 8] have shown that the degradation mechanisms can be classified according to their interval of characteristic amplitude. Identification of the damage mechanisms by fractography associated with the acoustic emission amplitudes was proposed (Fig. 4).

On the basis of these works, the mechanical behaviour can be analysed by several phases:

1st phase. The mechanical behaviour is characterised by the straight part of the load curve up to point NL, which corresponds to the damage initiation stage, and it is associated with a weak acoustic emission (very weak growth of the cumulative A.E. whose amplitude of the acoustic signals expressed by the first bursts of events is around 40 dB). This signal type expresses the presence of micro-cracks in the matrix as shown by Gong *et al.* and Meraghni *et al.* [7, 8].

2nd phase. This always starts with a displacement from approximately 0.6 to 0.8 mm whatever the $\pm\theta$ sequence used and is associated with the beginning of the non-linearity of the load curve. In this phase, the acoustic emission is more active than in the preceding phase. Thus, a phenomenon emitting around 65 dB was added to the phenomenon of interface fracture. Visual observations *in-situ* revealed that only at this loading stage does the phenomenon of bleaching on the extremely tense face of the specimen occur followed by transverse micro-cracks.

3rd phase. Its beginning shows a strong inflection of the cumulative A.E. curve. It presents a phenomenon very short in time (almost instantaneous) but very dissipative. Micro-cracks and transverse fracture by flexure occur at the initial crack tip during loading. This damage develops in the resin until a critical size which is necessary for the delamination to propagate.

4th phase. In a manner similar to that in the 3rd phase, the beginning shows also a strong inflection of the curve of cumulative A.E. curve. Using observations *in-situ*, the beginning of this phase is identified as the start of macroscopic delamination. The remainder of this phase presents the phenomenon of delamination propagation associated with all the mechanisms observed in the preceding phases.

Following what has just been described above, it appears very clearly that the composites $\pm\theta$ loaded in mode II by flexure experience very dissipative kinds of damage (transverse cracks) before delamination. A transverse crack is perpendicular to the direction of the propagation; it cannot thus be assimilated to a pseudo-length of crack such as Irwin has proposed for the decohesion zone. Thus, for our material, the application of linear elastic fracture mechanics requires a larger thickness than those likely to be standardised. The weak thickness makes material very sensitive to transverse cracking.

Values of the energy release rate noted $G_{\mathrm{IIC}}^{\mathrm{C}}$, $G_{\mathrm{IIC}}^{\mathrm{D}}$ and $G_{\mathrm{IIC}}^{\mathrm{cr}}$ (respectively given at instability (M), at the point of delamination starting (D) identified by the acoustic emission and at the point proposed by Carlsson *et al.* [6]) are summarised in Table 5. These values seem lower than envisaged: this is due to the fact one has not taken into account shearing, although this is amplified by transverse cracking. On the

Table 5.
G_{IIC} values

Sequences	G_{IIC}^{C} (M) (kJ/m^2)	G_{IIC}^{D} (D) (kJ/m^2)	G_{IIC}^{cr} (kJ/m^2)
$\pm 15°$	2.06	1.70	1.69
$\pm 30°$	1.92	1.60	1.52
$\pm 45°$	1.53	1.44	0.80

other hand, it should be stressed that these values correctly express the chronology of the damage phenomena.

Because the start of the delamination occurs shortly after the transverse fracture of the tense mid-plane ply, it is thus more advisable to calculate the dimensions of the structures by using the energy release rate at the point F. This point shows the transition between a bleaching phenomenon and the transverse cracks as detected by acoustic emission which underline the usefulness of this detecting method. The angle θ orientation seems to have a significant influence on the energy release rate whatever the point considered.

The absence of the G_{II}^{NL} values of the sequence $\pm 60°$ in Table 5 is due to the fact that this sequence practically does not have delamination except for ratios a_0/L very near unity and whose stress field at the head of initial crack is completely modified.

It appears from these observations reported above that the behaviour of angle-ply laminates is more complex than that of unidirectional materials. The bleaching phenomenon and the low specimen stiffness involve large displacement and non-linear behaviour which may invalidate the fracture mechanics concepts. These remarks assign to optimise a specimen dimensions as it discussed below.

4. SPECIMEN OPTIMISATION

The use of the concepts of linear elastic fracture mechanics is valid only in the case of a linear elastic behaviour with small displacements. Their application requires a check on two behaviour conditions in order:

- to avoid a non-linearity resulting from great displacements,
- to avoid a non-linearity of material or fracture by flexure.

On this subject, Carlsson *et al*. [6] presented an analysis based on the beam theory allowing the calculation of the dimensions of specimen ENF.

The first condition results in a maximum value of the slope y'_a, at the loading point. The acceptable displacement (δ_a) corresponding to y'_a can be calculated from equation (2):

$$\left(\frac{dy}{dx}\right) = \frac{3(L^2 + 3a^2)\delta}{2L^3 + 3a^3}. \tag{2}$$

Critical displacement of the fracture initiation is given by the relation (3):

$$\delta_c = \frac{2L^3 + 3a^3}{6a}\sqrt{\frac{G_{IIC}}{E_1 h^3}}. \tag{3}$$

The condition $\delta_c \leqslant \delta_a$ allows us to optimise the specimen dimensions by combining the equations (2) and (3).

For example, if the thickness h is the parameter which controls the specimen behaviour, we have

$$h \geqslant \sqrt{\frac{G_{IIC}(L^2 + 3a^2)^2}{4(y'_a)^2 \cdot a^2 \cdot E_1}}, \tag{4}$$

where G_{IIC} is the energy of initiation of the propagation; L is the half-length of specimen; a is the initial crack length and E_1 is the flexure modulus in the longitudinal direction.

For the second condition, optimisation will be done according to the permissible strain of the flexure. For a ratio $a/L < 0.5$, if there is a fracture by flexure, it occurs in the median section between the supports, where the maximal strain is given by equation (5)

$$\varepsilon_m = \frac{6Lh\delta}{2L^3 + 3a^3}. \tag{5}$$

In the same way as for the first condition, an optimisation thickness gives

$$h \geqslant \frac{L^2 G_{IIC}}{a^2 \varepsilon_{ma}^2 E_1}, \tag{6}$$

where ε_{ma} is the permissible strain of flexure.

A study by finite elements realised by Mall and Kochhar [9] showed that the analysis in linear elasticity can be used if the critical displacement does not exceed 1.5 times the total thickness of the specimen ($\delta \leqslant 3/2(2h)$), otherwise the G_{II} value will be overestimated.

In the same way as for specimen ENF, it is possible to use the non-linearity conditions for specimen ELS used in this study. In the case of non-linearity due to great displacements, acceptable displacement (δ_a) can be calculated by equation (7) for an acceptable slope y'_a.

$$\frac{dy}{dx} = \frac{3(3a^2 + L^2)}{2(3a^3 + L^3)}\delta. \tag{7}$$

The starting critical displacement is given by the relation (8):

$$\delta_c = \frac{L^3 + 3a^3}{3a}\sqrt{\frac{G_{IIC}}{E_1 h^3}}. \tag{8}$$

Table 6.
Mechanical and energy characteristics of the various sequences

Sequence	E_1 (GPa)	ε_{ma} 10^{-3}	G_{IIC} (kJ/m^2) st.d
UD	44.110	24.55	
±15°	38.560	9.95	
±30°	26.939	6.2	2.5
±45°	18.354	4	
±60°	16.432	2.53	

Combining the equations (7) and (8), the condition $\delta_z \leqslant \delta_a$ allows us to optimise the thickness (h) with relation (9):

$$h \geqslant \sqrt[3]{\frac{G_{IIC}(L^2+3a^2)^2}{4(y'_a)^2 a^2 E_1}}. \tag{9}$$

In the case of non-linearity due to the fracture by flexion, optimisation is to be done according to the acceptable strain of the fracture by flexure. For a ratio $a/L < 0.5$, if there is a fracture by flexure, it occurs on the cantilever where the strain is maximum and is given by:

$$\varepsilon_m = \frac{3Lh\delta}{L^3+3a^3}. \tag{10}$$

The fracture by flexure can be avoided using the optimal thickness h. It is the same relation as for specimen ENF:

$$h \geqslant \frac{L^2 \cdot G_{IIC}}{a^2 \varepsilon_{ma}^2 E_1}. \tag{11}$$

Optimisation by the application of the non-linearity conditions thus requires the knowledge of the following parameters: G_{IIC} (the energy release rate in mode II), ε_{ma} (fracture strain of material) and E_1 (the longitudinal modulus of elasticity by flexure). It should be noted that only G_{IIC} (2.5 kJ/m^2) is intrinsic to the laminate material whatever the orientation angle of the plies. On the other hand, ε_{ma} and E_1 depend on the orientation of the plies and are summarised in Table 6. The ε_{ma} values are calculated by application of the interactive criterion of Tsaï. As for the E_1 values, they are determined by the laminate theory.

A numerical application for the unidirectional laminate in this study whose $G_{IIC} = 2.5$ kJ/m^2, $\varepsilon_{ma} = 24.55 \times 10^{-3}$, $E_1 = 44110$ MPa, $h = 2.4$ mm, $\delta_c = 3h$ and $a_0/L = 0.5$ have given the lengths of the following specimens:

$L \leqslant 67$ mm for the 1st condition of non-linearity (great displacements),

$L \leqslant 42$ mm for the 2nd condition of non-linearity (fracture by flexure).

The 2nd condition of non-linearity proves more severe and needs to be used for any optimisation. A length of $L = 40$ mm appears very practical in the case of the specimen ENF of which the total length will be of 80 mm. However, in the case of

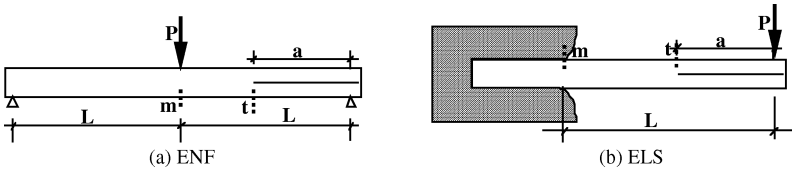

Figure 5. Dangerous sections in specimens ENF and ELS.

specimen ELS, this length is insufficient because of the obstruction of the assembly. It should be also noted that this length was calculated for a unidirectional laminate. Consequently, the application of the same condition to laminates $\pm\theta$ (with $\theta > 0°$) requires certainly lower lengths (L).

The application of the equation (11) allows to determine, for a thickness, h, and a given ratio (a/L), the minimal strain ε_{m} which causes the fracture by delamination. Thus, as long as $\varepsilon_{\mathrm{m}} < \varepsilon_{\mathrm{ma}}$ the fracture is done completely by delamination. On the other hand, if $\varepsilon_{\mathrm{m}} \gg \varepsilon_{\mathrm{ma}}$, the fracture is done completely by flexure. As for the cases where ε_{m} is higher but very near to $\varepsilon_{\mathrm{ma}}$, the process of fracture is the combination of the fracture by flexure and delamination. In fact in this intermediate case, the fracture initiation is by flexure (transverse fracture of first ply, extremely tense) then the delamination occurs under the effect of amplification of shear stress after the fracture of the first ply. This calculation and checking procedure must be carried out for all the stacking sequences and for a ratio (a/L) going from 0 to 1.

However, if for $a/L < 0.5$, the maximal strain is at the point, m (Fig. 5); it is not the same for $a/L > 0.5$ where the maximal strain is at the head of the initial crack (point t). The relation between the two strains on the points m and t is treated by the usual theory of beams.

In this case, the stresses at the points (m) and (t) are given by:

$$\sigma_{\mathrm{m}} = \frac{3PL}{4bh^2} \quad \text{and } \sigma_{\mathrm{t}} = \frac{3Pa}{2bh^2} \quad \text{for ENF specimen,}$$

$$\sigma_{\mathrm{m}} = \frac{3PL}{2bh^2} \quad \text{and } \sigma_{\mathrm{t}} = \frac{3Pa}{bh^2} \quad \text{for ELS specimen,}$$

therefore, $\sigma_{\mathrm{t}} = 2a/(L)\sigma_{\mathrm{m}}$ for the two specimen types and whatever the ratio (a/L). Consequently, for the two specimen types $\varepsilon_{\mathrm{t}} = 2a/(L)\varepsilon_{\mathrm{m}}$.

Thus, for any ratio $a/L < 0.5$ and $\varepsilon_{\mathrm{t}} < \varepsilon_{\mathrm{m}}$, the check on the fracture by flexure must be done on the point m where the section is more dangerous. On the other hand, for any ratio $a/L > 0.5$ and $\varepsilon_{\mathrm{t}} > \varepsilon_{\mathrm{m}}$, the check on the fracture by flexure is done on the point t.

The minimal values ε_{m} (for $a/L < 0.5$) and ε_{t} (for $a/L > 0.5$) causing the fracture by delamination for a thickness $h = 2.4$ mm are presented in Table 7. It is necessary to note that for a ratio $a/L = 0$, the strain ε_{m} is infinite. That means that for such ratio $a/L = 0$, the specimen does not contain any initial crack and the fracture initiation is done by flexure on the point m without delamination risk in the median plan of the end of the specimen.

Table 7.
Minimal strains ensuring the fracture by delamination

$\varepsilon_m \times 10^{-3}$						$\varepsilon_t \times 10^{-3}$
Sequences	$a/L = 0$	$a/L = 0.2$	$a/L = 0.3$	$a/L = 0.4$	$a/L = 0.5$	$a/L > 0.5$
UD	∞	24.55	16.20	12.10	9.72	9.72
$\pm 15°$	∞	25.60	17.32	12.99	10.40	10.40
$\pm 30°$	∞	31.10	20.73	15.54	12.00	12.00
$\pm 45°$	∞	37.66	25.11	18.83	15.06	15.06
$\pm 60°$	∞	39.81	26.54	19.90	15.90	15.90

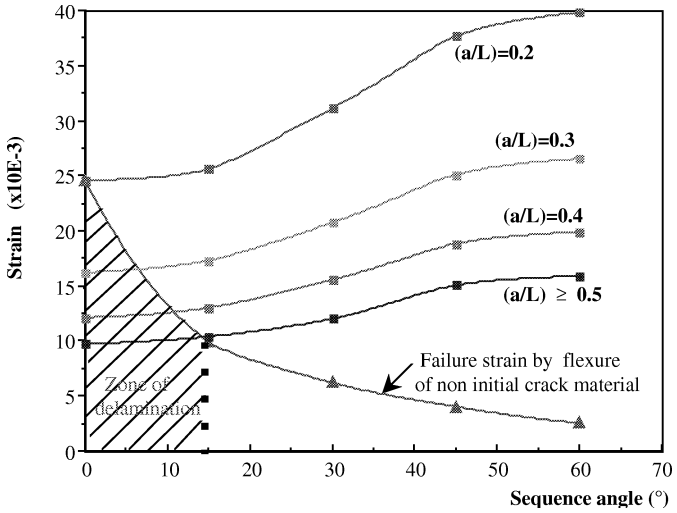

Figure 6. Abacus giving the fracture strains by flexure according to the orientation angle of the plies and to the a/L ratio.

The ε_m value decreases with the increase of the ratio a/L and increases with the orientation angle of the plies. However, when the ratio $a/L > 0.5$ although the strain ε_m continues to decrease with the increase of ratio a/L, the strain ε_t remains constant. It keeps the values corresponding to the ratio $a/L = 0.5$ whatever the value of $a/L \geqslant 0.5$.

A comparison between the minimal strains ensuring the fracture by delamination and the fracture strains by flexure is illustrated by Fig. 6. It appears clearly that the fracture initiation is always done by flexure in the following cases:

- for a ratio $a/L < 0.2$ and whatever the orientation angle of the plies (even for the UD).
- for all $\theta \geqslant 15°$, whatever the ratio a/L.

As for the fracture by delamination, it occurs when the conditions of the angle θ and the ratio a/L are those delimited by the contour of the shaded zone. In fact, when θ is lower than 15°, any couple $(\theta, a/L)$ which is below the curve of failure

Table 8.
Minimal thickness ensuring the fracture by delamination

Sequence	Half-thickness of the specimens				
	$a/L = 0$	$a/L = 0.2$	$a/L = 0.3$	$a/L = 0.4$	$a/L = 0.5$
UD	∞	2.30	1.04	0.58	0.38
±15°	∞	16.37	7.27	4.10	2.62
±30°	∞	60.00	26.82	15.09	9.65
±45°	∞	212.00	94.60	53.20	34.05

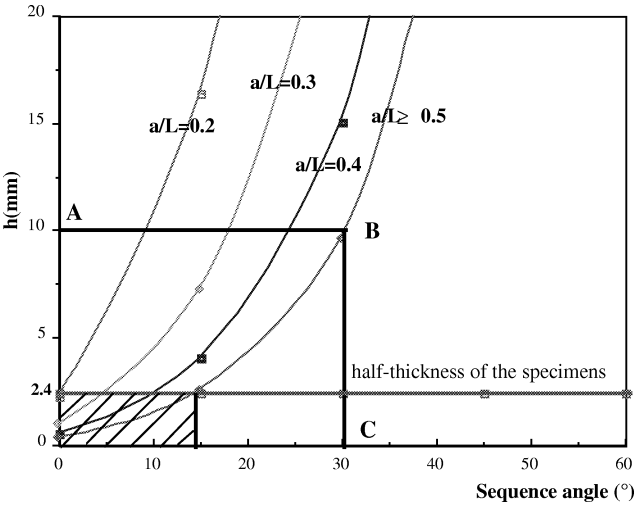

Figure 7. Minimal thickness ensuring the fracture by delamination.

strain by flexure of undamaged material, causes a delamination without transverse cracking. For example, for $\theta = 10°$ all the ratios $a/L \geqslant 0.4$ cause a fracture by delamination alone (without transverse cracking).

The same remark can be made for thickness optimisation of the specimens. To this effect, the application of relation 6 allows us to determine, for a given fracture strain by flexure and a given ratio a/L, the necessary minimal thickness to ensure a fracture by delamination. Table 8 summarises the minimal thickness values h necessary for the all sequences of the stratification and a ratio a/L from 0 to 1. The comparison between these results and the real thickness of material in this study is illustrated by Fig. 7. The analysis of the various curves of this figure makes it possible to explain the fracture process of the $\pm\theta$ according to the thickness of the specimens and to the ratio a/L.

We notice clearly the close link between the angle θ, the ratio a/L and the thickness h of material. The fracture by delamination can be obtained only with an optimal choice between these three parameters. For example for $\theta = 20°$ associated

with a ratio $a/L = 0.4$, the adequate thickness h to cause a fracture by delamination is lower or equal to 0.6 mm whereas it can almost double for a ratio $a/L = 0.3$.

As for the cases of material in this study ($h = 2.4$ mm), the fracture takes place by simple delamination for any couple $(\theta, a/L)$ pertaining to the small hatched rectangle. Thus, for all studied sequences, fracture cannot occur only by delamination if they are loaded in mode II by flexure, which was checked in experiments. All these results can contribute to the standardisation of this test type which can be more difficult to implement than that of mode I.

5. CONCLUSIONS

The angle orientation θ has a significant influence on the value of the energy release rate G_{IIC}. This value also depends on the load considered (load of end of linearity P_{N}, load of delamination P_{D}, or average load).

The tests of Mode II on specimens ENF and ELS with angles $(\pm\theta)$ require a preliminary geometrical optimisation in order to avoid cracking away from the mid-plane which dissipates energy. This study shows the correlation between the angle θ, the ratio a/L and the thickness h of material. For a 5 mm thickness the fracture cannot be done by delamination only without transverse cracking for the studied sequences of stratification.

In fact, a bleaching phenomenon and transverse cracks occur well before delamination. This damage mechanism generates a dissipation of energy which involve a reduction of the strain energy release rate of delamination cracks.

These results show that the linear elastic fracture mechanics concepts (LEFM) is unsatisfactory for characterising the delamination of angle-ply laminates $(\pm\theta)$ in mode II for weak specimen thickness. Acoustic emission is a very useful technique to detect damage mechanisms which involve microcracks and delamination.

REFERENCES

1. D. J. Nicholls and J. P. Gallagher, Determination of GIC in angle ply composites using a cantilever beam test method, *J. Reinf. Plast. Compos.* **2**, 2–17 (1983).
2. H. Chai, The characterization of mode I delamination failure in non-wowen, multidirectional laminates, *Composites* **15** (4), 277–290 (1984).
3. P. Robinson and D. Q. Song, A modified DCB specimen for mode I of multidirectionnel laminates, *J. Compos. Mater.* **26** (11), 1554–1577 (1992).
4. A. J. Russel and K. N. Street, Factors affecting the interlaminar fracture energy of graphite/epoxy laminates, in: *4th Int. Conf. on Compos. Mater. (ICCM VI)*, Tokyo, pp. 279–286 (1982).
5. J. Whitney and L. M. Pinnel, Characterization of interlaminar mode II fracture using beam specimens, in: *Science and Technology of Composite Materials (ECCM IV)*, Stuttgart, pp. 865–868 (1990).
6. L. A. Carlsson, J. W. Gillepsie, Jr. and R. B. Pipes, On the analysis and design of End Notched Flexure (END) specimen for mode II testing, *J. Compos. Mater.* **20**, 594–604 (1986).

7. X. L. Gong, A. Laksimi and M. L. Benzeggagh, Nouvelle approche de l'émission acoustique et son application à l'identification des mécanismes d'endommagement dans les matériaux composites, *Revue des composites et des Matériaux Composites Avancées* **8** (1), 7–23 (1998).
8. F. Meraghni, S. Benmedakhene and M. L. Benzeggagh, Identification and modeling of damage mechanisms in short glass fiber reinforced polypropylene, in: *ICCM10*, Vancouver, Vol. I, pp. 359–366 (1995).
9. Mall and Hochhar, Finite-element analysis of end notch flexure specimens, *J. Compos. Technol. Research* **8** (2), 54–57 (1986).
10. A. Ahmed Benyahia, Etude des mécanismes de délaminage sous l'effet de contrainte complexes générées par des sollicitation simple d'ouverture et de cisaillement dans les stratifiés $\pm\theta$, Thesis Université de Technologie de Compiègne, No. 1040 (1997).